

Theoretical Analysis of Magnetic Tunneling Transistor as a Novel Hydrogen Gas Sensor Based on Spintronic

Vahdat NAZERIAN*

Alireza SALEHI

Laboratory of Device Fabrication, Department of Electrical Engineering, K.N. Toosi, University of Technology, P.O. Box 16315-1355, Seyed Khandan, Tehran, IRAN

*Corresponding Author

e-mail:nazerian@eetd.kntu.ac.ir

Received : September 19, 2011

Accepted : October 24, 2011

Abstract

A novel approach has been presented using a sensor model to study the sensing response of magnetic tunneling transistor (MTT) as a highly sensitive hydrogen gas sensor. We have shown that when MTT was exposed to hydrogen gas the magnetization of upper ferromagnetic layer (emitter) decreased resulting in a decrease in spin polarization of the electrons in the layer which creates higher collector current in the circuit. We conducted a sensor model using simulation of the device to examine the effect of the Schottky barrier of the collector-base junction on the sensor response towards various hydrogen concentrations. An interesting result of the simulation was a very high response of 13.7 times increase in sensing response of the device with Schottky barrier subjected to a very low concentration of hydrogen compared to the device without Schottky barrier, exhibiting the high performance of MTT sensor for detection of very low hydrogen concentrations. Further, the relation between the response of MTT sensor and the thickness of the insulator barrier of emitter-base magnetic tunneling junction was also investigated. The sensing response of MTT sensor was inversely related to the insulator barrier thickness and a higher gas response was obtained for thinner insulator layers.

Keywords: Sensing Response; Magnetic Tunneling Transistor (MTT); Ferromagnetic Layer; Spin Polarization; Schottky Barrier

INTRODUCTION

In recent years gas sensors using different materials and different techniques have been vastly investigated [1-3], but due to constraints in low gas concentration response and low operating temperatures new semiconductor structures are needed to be investigated. It is well known that in normal electronic the charge of carriers for controlling the electric current is used. However, there are new devices in which the spin of carriers is used for controlling the electric current [4-6]. The new approach is known as spintronic and the phenomenon is used in this study for gas detection. When some gases exposed to the surface of ferromagnetic layers the magnetization properties of the layers are affected significantly [7-9]. In our previous work [10] we fabricated a magnetic Ni/n-Si Schottky diode as hydrogen gas sensor so that the exposure of the gas to the surface of ferromagnetic Ni layer affected the magnetization of the layer significantly and so, a considerable improvement in sensing response of the device towards hydrogen gas was achieved. Hence, we will be able to detect the hydrogen gas if the changes of the magnetization characteristics of the layers are measured properly. We believe that there is a reason to investigate new structures of ferromagnetic layers for gas detection. So, in the present paper we report that magnetic tunneling transistor (MTT) can be used as a novel hydrogen gas sensor. To our knowledge, works on MTT structure as a gas sensor has not yet been published.

Presentation of MTT Gas Sensor

It is known that in the spin device of MTT the upper ferromagnetic layer (emitter) which acts as a spin filter propagates the spin-polarized electrons by tunneling across the insulator barrier into the inner ferromagnetic film (base) serving as a spin detector [11-13]. The n-type Si semiconductor (collector) forms Schottky barrier at the collector-base interface. When a current is injected by tunneling across the emitter-base barrier, some electrons will pass straight across the base into the collector causing a current flow between the collector and the base. These are called "hot" electrons because their energy is well above the Fermi level of the metal and they have enough energy to overcome the Schottky barrier at the collector-base interface. In contrast, electrons that scatter inelastically in the gap lose energy and usually are accumulated in the base [14,15]. In such structure we are able to control the collector current (I_c) with a change in amount of the magnetization of each ferromagnetic layer (emitter or base). Figure 1 shows the explanation of gas sensing procedure using MTT structure. In Figure 1(a), the situation of the sensor in clean air is shown. The tunneling probability of electrons across the tunnel barrier is low before the gas exposure because the magnetization directions of two ferromagnetic layers (emitter and base) are definitely anti parallel. Therefore little spin-polarized electrons are injected from the emitter into the base. Since these electrons lose their energy while crossing the base region they can not overcome the Schottky barrier at the collector-base interface

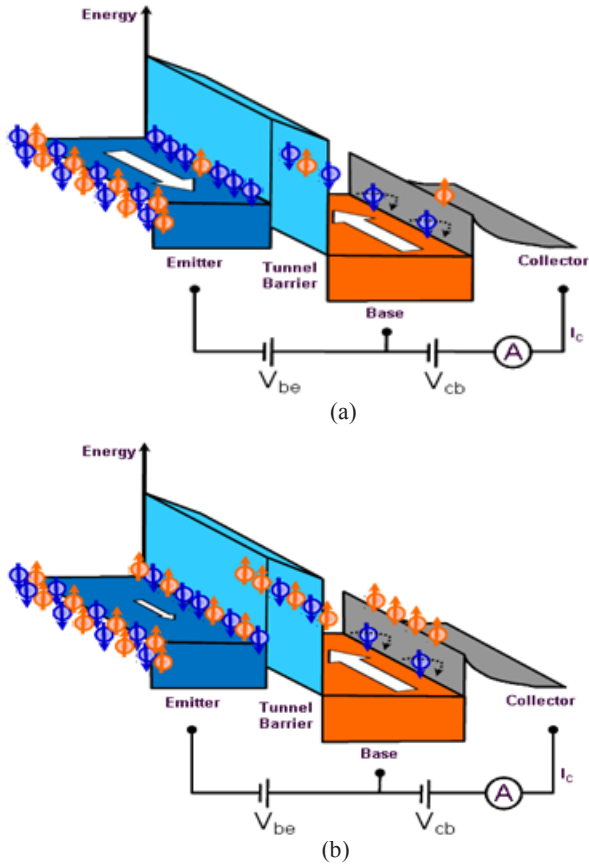


Fig.1. Presentation of MTT gas sensor proposed in the present study: (a) Before the gas exposure (b) After the gas exposure.

and are scattered back [Figure 1(a)]. As a result no electric current flows in collector of the circuit. Now in exposure of hydrogen gas [Figure 1(b)], the arrangement of the magnetic domains in emitter layer is changed by surface adsorption of the hydrogen atoms resulting in a reduction of the emitter layer magnetization. Therefore, the spin-polarization of electrons in the emitter region decreases which causes an increase in density of the opposite spin states (the states have the spin anti parallel to the magnetization direction of the emitter or parallel to the magnetization direction of the base) in that region. Thus, the tunneling probability of electrons across the insulator barrier increases significantly and the spin-polarized electrons are injected from the emitter into the base. The base width is very thin namely less than the diffusion length of the carriers and so the electrons injected by tunneling into the base pass across the base [16]. Because these electrons have the spin parallel to magnetization direction of the base they keep the energy while crossing the base and pass the Schottky barrier at the collector-base interface as shown in Figure 1(b). So, the collector current of the circuit (I_c) increases drastically which is used for detection of hydrogen gas in the ambient.

If we record the change of the collector current as sensing response of the sensor then the Equation (1) can be used for calculations [10]:

$$S\% = \left(\frac{I_g}{I_a} - 1 \right) \times 100 \quad (1)$$

Where I_{cg} and I_{ca} denote the collector current at identical bias voltage in presence of hydrogen gas and in clean air,

respectively. As mentioned before we currently are working on fabrication of the proposed sensor but prior to that we report the results of the simulation as follows.

Analysis of MTT Gas Sensor

It should be noted that some effective parameters show a crucial role on the response of the proposed sensor towards test gas. The number of the electrons reaching the collector terminal increases exponentially with mean free path of the electrons in the emitter and base ferromagnetic layers. This is significantly dependent on amount of the magnetization of the layers [17]. The electrons will pass the tunnel barrier of the emitter-base junction and the transmission probability of the tunneling event declines exponentially with tunnel barrier thickness with a time constant depending on potential barrier height [18,19]. Moreover, some other factors such as the base width and the Schottky barrier of the collector-base junction (Φ_{cb}) are important in the response of MTT sensor. The analysis of the effect of each parameter by itself can be useful in optimum sensor design. In the present paper we studied the effect of Φ_{cb} , tunnel barrier thickness and hydrogen concentration on the sensing response of MTT gas sensor. For this purpose the sensor was considered to have the collector current towards hydrogen gas as a function of insulator thickness in two different samples with Schottky barrier and without Schottky barrier and so, we calculated the sensing response of the sensor using the Equation (1), where other parameters were assumed to be constant. MATLAB software was used to obtain the sensing characteristics of the sensor in response to hydrogen gas. First in Figure 2, we studied the gas sensor without Schottky barrier which is a magnetic tunneling junction (MTJ) [11,12].

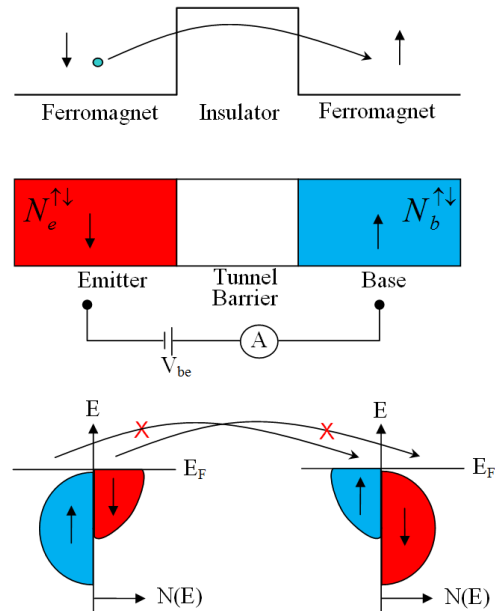


Fig.2. Schematic picture of carrier tunneling and density of electron states at Fermi level (E_F) in the emitter-base junction.

The tunneling current density of the carriers (J_T) between emitter-base magnetic tunneling junction can be calculated using [20]:

$$J_T \propto N_e^{\uparrow\downarrow} \cdot N_b^{\uparrow\downarrow} \cdot e^{\frac{N_e^{\uparrow\downarrow} \cdot N_b^{\uparrow\downarrow}}{\alpha} \cdot V_{be}} \rightarrow J_T = k_T \cdot N_e^{\uparrow\downarrow} \cdot N_b^{\uparrow\downarrow} \cdot e^{\frac{N_e^{\uparrow\downarrow} \cdot N_b^{\uparrow\downarrow}}{\alpha} \cdot V_{be}} \quad (2)$$

Where $N_e^{\uparrow\downarrow}$ and $N_b^{\uparrow\downarrow}$ are densities of the electron states with up and down spins in the emitter and base sides of the emitter-base junction, respectively. V_{be} is bias voltage of the junction, α is a factor related to the thickness of the insulator barrier and k_T is proportion factor of the tunneling. So, we can calculate the electric current (I) using:

$$\begin{aligned} I &= A.J_T = A.k_T.N_e^{\uparrow\downarrow}.N_b^{\uparrow\downarrow}.e^{\frac{N_e^{\uparrow\downarrow}.N_b^{\uparrow\downarrow}.V_{be}}{\alpha}} \\ &= A.k_T.N_e^{\uparrow}.N_b^{\uparrow}.e^{\frac{N_e^{\uparrow}.N_b^{\uparrow}.V_{be}}{\alpha}} + A.k_T.N_e^{\downarrow}.N_b^{\downarrow}.e^{\frac{N_e^{\downarrow}.N_b^{\downarrow}.V_{be}}{\alpha}} \end{aligned} \quad (3)$$

Where A is surface area of the junction. To determine I we should measure $N_e^{\uparrow\downarrow}$ and $N_b^{\uparrow\downarrow}$ before and after the gas exposure. We assume that the density of states of total electrons in emitter and base are N_e and N_b , respectively and $N_e=N_b=N$. Now if we assume that with hydrogen gas exposure the densities of electron states with up and down spins near the Fermi level in emitter region changes as a result of a change in emitter magnetization then N_e^{\uparrow} and N_e^{\downarrow} in emitter region can be calculated using:

$$\begin{cases} N_e^{\uparrow} : \frac{N}{10} \rightarrow \frac{N}{2} \\ N_e^{\downarrow} : \frac{9N}{10} \rightarrow \frac{N}{2} \end{cases} \Rightarrow \begin{cases} N_e^{\uparrow} = f_e^{\uparrow}(g) = \frac{4N}{10} \cdot \frac{g}{G_0} + \frac{N}{10} \\ N_e^{\downarrow} = f_e^{\downarrow}(g) = \frac{-4N}{10} \cdot \frac{g}{G_0} + \frac{9N}{10} \end{cases} \quad (4)$$

Where g represents hydrogen gas concentration in ppm and G_0 denotes the saturation concentration of hydrogen gas which causes the elimination of the magnetization of emitter region and is dependent on different parameters such as the type of test gas, the thickness and the magnetization of ferromagnetic layer exposed to test gas. Further, with gas exposure the magnetization of the base region remains constant and hence N_b^{\uparrow} and N_b^{\downarrow} in the base region can be calculated using:

$$\begin{cases} N_b^{\uparrow} : \frac{8N}{10} \rightarrow \frac{8N}{10} \\ N_b^{\downarrow} : \frac{2N}{10} \rightarrow \frac{2N}{10} \end{cases} \Rightarrow \begin{cases} N_b^{\uparrow} = f_b^{\uparrow}(g) = \frac{8N}{10} \\ N_b^{\downarrow} = f_b^{\downarrow}(g) = \frac{2N}{10} \end{cases} \quad (5)$$

Substituting of the values of the Equation (4) and Equation (5) into the Equation (3) we obtain the electric current in presence of gas (I_g) using:

$$\begin{aligned} I_g &= I_g^{\uparrow} + I_g^{\downarrow} \\ &= A.k_T \left(\frac{4N}{10} \cdot \frac{g}{G_0} + \frac{N}{10} \right) \cdot \left(\frac{8N}{10} \right) e^{\frac{\left(\frac{4N}{10} \cdot \frac{g}{G_0} + \frac{N}{10} \right) \cdot \left(\frac{8N}{10} \right) \cdot V_{be}}{\alpha}} \\ &\quad + A.k_T \left(\frac{-4N}{10} \cdot \frac{g}{G_0} + \frac{9N}{10} \right) \cdot \left(\frac{2N}{10} \right) e^{\frac{\left(\frac{-4N}{10} \cdot \frac{g}{G_0} + \frac{9N}{10} \right) \cdot \left(\frac{2N}{10} \right) \cdot V_{be}}{\alpha}} \end{aligned} \quad (6)$$

To calculate the amount of the electric current in clean air (I_a) we should substitute $g=0$ in the Equation (6). We then obtain:

$$\begin{aligned} I_a &= I_a^{\uparrow} + I_a^{\downarrow} \\ &= A.k_T \left(\frac{N}{10} \right) \cdot \left(\frac{8N}{10} \right) e^{\frac{\left(\frac{N}{10} \right) \cdot \left(\frac{8N}{10} \right) \cdot V_{be}}{\alpha}} + A.k_T \left(\frac{9N}{10} \right) \cdot \left(\frac{2N}{10} \right) e^{\frac{\left(\frac{9N}{10} \right) \cdot \left(\frac{2N}{10} \right) \cdot V_{be}}{\alpha}} \end{aligned} \quad (7)$$

At a fixed bias voltage (V_{be}) of 1V if we denote $\frac{N^2}{\alpha}$ as η then the response of MTJ gas sensor in emitter-base junction (S_0) can be calculated using:

$$\begin{aligned} S_0 \% &= \left(\frac{I_g}{I_a} - 1 \right) \times 100 = \\ &= \left(\frac{\left(4 \cdot \frac{g}{G_0} + 1 \right) \cdot (8) e^{\left(\frac{4}{10} \cdot \frac{g}{G_0} + \frac{1}{10} \right) \cdot \eta} + \left(-4 \cdot \frac{g}{G_0} + 9 \right) \cdot (2) e^{\left(\frac{-4}{10} \cdot \frac{g}{G_0} + \frac{9}{10} \right) \cdot \eta}}{8 e^{\frac{8}{100} \cdot \eta} + 18 e^{\frac{18}{100} \cdot \eta}} - 1 \right) \times 100 \end{aligned} \quad (8)$$

Since η is inversely related to α , and α denotes the tunneling factor which is related to the thickness of insulator barrier, so, we can consider η is inversely defined by the thickness of tunneling barrier if the other parameters are assumed to be constant.

To analyze the effect of the Schottky barrier of Φ_{cb} on the sensing response of the sensor we used the electron traveling factor (γ) over the Schottky barrier of Φ_{cb} for the electrons in two different positions of spin up and spin down as shown in Figure 3. In this figure γ^{\uparrow} and γ^{\downarrow} denote the electron traveling factors in spin up and spin down conditions, respectively. So, we can calculate γ^{\uparrow} and γ^{\downarrow} using:

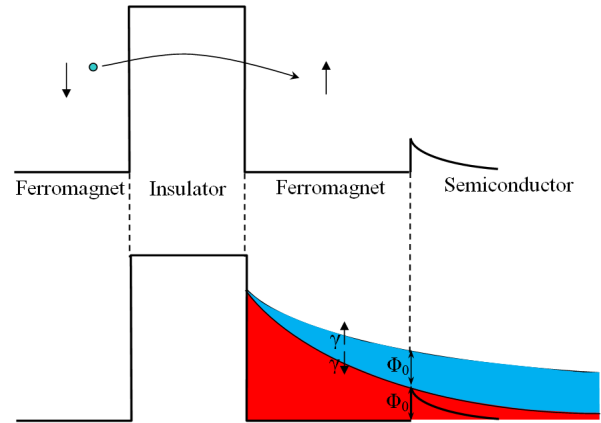


Fig.3. Schematic picture of Schottky barrier of Φ_{cb} and its effect on sensing response.

$$\Phi_{cb}=0 : \begin{cases} \gamma^{\uparrow} = 1 \\ \gamma^{\downarrow} = 1 \end{cases} \quad \Phi_{cb} \neq 0 : \begin{cases} \gamma^{\uparrow} = 1 \\ \gamma^{\downarrow} = 0 \end{cases} \quad (9)$$

Where Φ_0 is barrier height of Ni/n-Si Schottky contact if the collector and base sides of the junction are made of n-type Si semiconductor and ferromagnetic Ni metal layer, respectively and is calculated from the Equation (10) [21]:

$$\Phi_0 = (kT/q) \ln(A^*AT^2/I_s) \quad (10)$$

Where I_s is the saturation current; A , the contact area; A^* , the effective Richardson constant; T , the absolute temperature; k , the Boltzmann's constant and q , the elementary charge. It should be noted that the base region is narrow to such an extent that Φ_0 causes the travelling of down spin electrons to be obstructed as shown in Figure 3.

So, the collector current in presence of gas (I_{cg}) is obtained from:

$$\begin{aligned} I_{cg} &= I_{cg}^{\uparrow} + I_{cg}^{\downarrow} = \gamma^{\uparrow} I_g^{\uparrow} + \gamma^{\downarrow} I_g^{\downarrow} = 1 I_g^{\uparrow} + 0 I_g^{\downarrow} = I_g^{\uparrow} \\ &= A k_T \left(\frac{4N}{10} \cdot \frac{g}{G_0} + \frac{N}{10} \right) \cdot \left(\frac{8N}{10} \right) e^{\frac{(\frac{4N}{10} \cdot \frac{g}{G_0} + \frac{N}{10}) \cdot (\frac{8N}{10})}{\alpha} V_{bc}} \end{aligned} \quad (11)$$

To calculate the amount of the collector current in clean air (I_{ca}) we should substitute $g=0$ in the Equation (11). We then obtain:

$$\begin{aligned} I_{ca} &= I_{ca}^{\uparrow} + I_{ca}^{\downarrow} = \gamma^{\uparrow} I_a^{\uparrow} + \gamma^{\downarrow} I_a^{\downarrow} = 1 I_a^{\uparrow} + 0 I_a^{\downarrow} = I_a^{\uparrow} \\ &= A k_T \left(\frac{N}{10} \right) \cdot \left(\frac{8N}{10} \right) e^{\frac{(\frac{N}{10}) \cdot (\frac{8N}{10})}{\alpha} V_{bc}} \end{aligned} \quad (12)$$

The response of MTT gas sensor with Schottky barrier of Φ_0 (S_1) can be calculated using:

$$S_1 \% = \left(\frac{I_{cg}}{I_{ca}} - 1 \right) \times 100 = \left(4 \frac{g}{G_0} + 1 \right) e^{\frac{32}{100} \frac{g}{G_0} \eta} - 1 \times 100 \quad (13)$$

RESULTS AND DISCUSSION

Using the Equations (13) and (8), the response of MTT and MTJ sensors (S_1 and S_0 , respectively) towards various hydrogen gas concentrations from zero to saturation concentration (G_0) is shown in Figure 4. The thickness of the tunnel barrier was changed in three steps. Comparing the results shown in Figure 4, it is observed that the response of MTT sensor to hydrogen exhibits a significant increase compared to MTJ sensor. Curve 'f' shows that the MTT sensor exhibits much higher response to hydrogen gas, in contrast to the MTJ sensor with the same tunnel thickness (Curve 'c'). A response value of around 3310 was calculated for MTT sensor to G_0 of hydrogen with tunnel barrier thickness defined by $\eta=6$ (Curve 'f'), whereas a response value of 596 was obtained for MTJ sensor at the same conditions (Curve 'c'). This is a more than 5.5-fold increase of the sensing response of the sensor, exhibiting the high performance of the device for detection of hydrogen gas when Schottky barrier was used. Further, as shown in Curve 'e', the response of MTT sensor with thinner tunnel barrier thickness ($\eta=3$) towards hydrogen gas is much higher than that of MTT sensor with thicker barrier thickness ($\eta=1$) shown in Curve 'd'. The difference shows an increase of about 2 orders

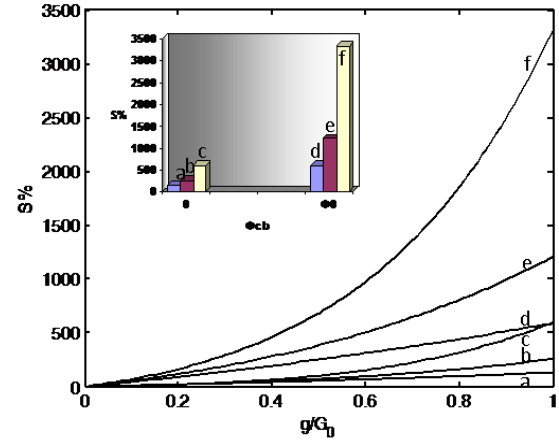


Fig.4. Sensing response of the sensors towards various hydrogen gas concentrations. Curves 'a', 'b' and 'c' show MTJ sensor with $\eta=1, 3$ and 6 , respectively and curves 'd', 'e' and 'f' show MTT sensor with $\eta=1, 3$ and 6 , respectively. The inset shows the sensing response of MTT and MTJ samples exposed to saturation concentration (G_0) of hydrogen.

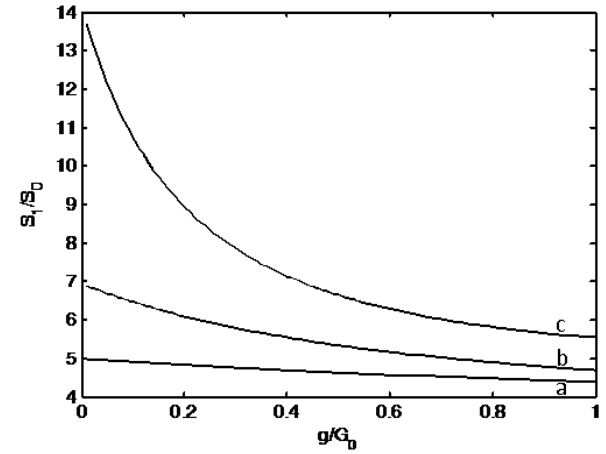


Fig. 5. Relative response of the sensors towards various hydrogen concentrations. $\eta=1, 3$ and 6 for curves 'a', 'b' and 'c', respectively.

of magnitude in response to G_0 of hydrogen gas. For the clarity of the changes, we summarized the results of the response to G_0 of hydrogen gas versus three different tunnel thicknesses for MTT and MTJ sensors in the inset of Figure 4. It is shown that both MTT and MTJ responses increase considerably with a decrease in tunnel barrier thickness and the response value of MTT samples towards hydrogen gas are more significant than those of MTJ devices.

In order to compare S_1 and S_0 , the relative response (S_1/S_0) towards various hydrogen concentrations obtained from the proportion of the Equations (13) and (8) is shown in Figure 5. It is obvious that a very high response of 13.7 times increase in sensing response of MTT device was achieved towards very low hydrogen gas concentration compared to MTJ device.

To characterize the variations of the response values of MTT and MTJ sensors with various tunnel thicknesses when exposed to different concentrations of hydrogen, we used the Equations (13) and (8). The results are shown in Figure 6. It is observed that the response values of both MTT and MTJ devices increase with increasing the hydrogen concentration. Further, the sensing response of MTT sensor towards hydrogen is much higher than that of MTJ sensor subjected to similar concentration of

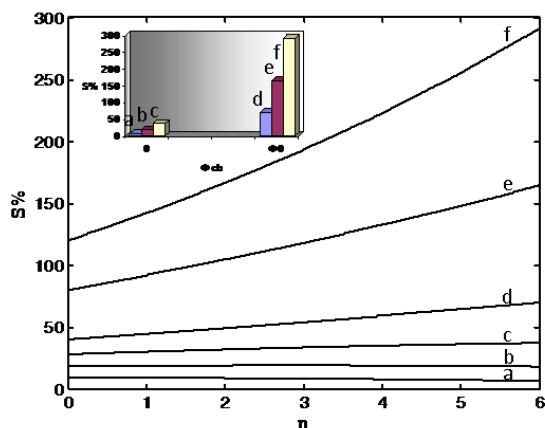


Fig.6. Sensing response of the sensors versus various tunnel barrier thicknesses. Curves 'a', 'b' and 'c' show MTJ sensor exposed to $g=0.1G_0$, $0.2G_0$ and $0.3G_0$ of hydrogen gas, respectively and curves 'd', 'e' and 'f' show MTT sensor exposed to $g=0.1G_0$, $0.2G_0$ and $0.3G_0$ of hydrogen, respectively. The inset shows the sensing response of MTT and MTJ samples with $\eta=6$.

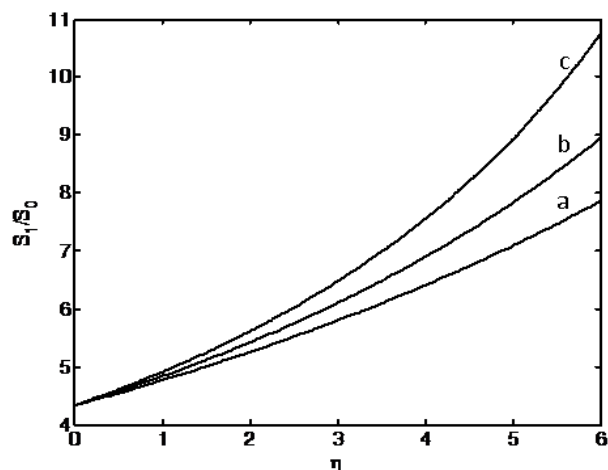


Fig.7. Relative response of the sensors versus various tunnel barrier thicknesses. $g=0.1G_0$, $0.2G_0$ and $0.3G_0$ of hydrogen gas for curves 'a', 'b' and 'c', respectively.

hydrogen. The trends in Figure 6 exhibit an excellent agreement with those of the sensing characteristics shown in Figure 4. The changes of the response values of MTT and MTJ samples at a fixed tunnel thickness versus three different hydrogen concentrations are shown in the inset of Figure 6. It is shown that both MTT and MTJ responses increased considerably with an increase in hydrogen concentration and MTT sensor exhibited much higher response compared to MTJ sensor.

For more clarity of the sensing response of MTT and MTJ devices versus various tunnel thicknesses, we obtained the relative response of the sensors (S_i/S_0) submitted to three different concentrations of hydrogen gas. The results were summarized in Figure 7. It is shown in Figure 7 that the relative response increased drastically with increasing the hydrogen concentration.

CONCLUSION

In conclusion, we proposed a new approach of gas sensing using a sensor model of MTT as a highly sensitive hydrogen

gas sensor so that the gas adsorption on the surface of the sensor causes a reduction of emitter magnetization and the MTT structure converts the changes of the magnetization characteristics into the collector current of the circuit (I_c) which is used for gas detection in the ambient. We studied the effect of Φ_{ob} on the response of the sensors towards various gas concentrations using simulation of the device. It was observed that the sensing response of MTT sensor towards hydrogen was much higher than that of MTJ sensor subjected to a very low gas concentration, exhibiting the high performance of MTT device for detection of very low concentrations of hydrogen gas at room temperature. Moreover, the effect of the tunneling barrier thickness on the sensing response of the sensor was also investigated. It was obvious that a higher gas response was obtained when we decreased the insulator barrier thickness.

So, using the appropriate design of MTT parameters, we propose it as a good candidate of hydrogen gas sensor.

Acknowledgements

The authors thank M. M. Lajvardi for his help in samples preparation and gas sensing measurements.

REFERENCES

- [1] Nicoletti S, Zampolli S, Elmi I, Dori L, Severi M. 2003. Use of different sensing materials and deposition techniques for thin film sensors to increase sensitivity and selectivity. *IEEE Sensors Journal*. 3:454-459.
- [2] Zhang T, Mubeen S, Myung NV, Deshusses MA. 2008. Recent progress in carbon nanotube-based gas sensors. *Nanotechnology*. 19:332001-1-332001-14.
- [3] Wang YD, Wu X, Zhou Z. 2000. Novel high sensitivity and selectivity semiconductor gas sensor based on the p + n combined structure. *Solid-State Electronics*. 44:1603-1607.
- [4] Barnas J, Fert A, Gmitra M, Weymann I, Dugaev VK. 2005. From giant magnetoresistance to current-induced switching by spin transfer. *Physical Review B*. 72:024426-1-024426-12.
- [5] Wolf SA, Awschalom DD, Buhrman RA, Daughton JM, von Molnár S, Roukes ML, Chtchelkanova AY, Treger DM. 2001. Spintronics: a spin-based electronics vision for the future. *Science*. 294:1488-1495.
- [6] Parkin SSP. 2002. Applications of magnetic nanostructures. *Advances in Condensed Matter Science*. 3:237-277.
- [7] Oba Y, Sato T, Shinohara T. 2006. Gas adsorption on the surface of ferromagnetic Pd nanoparticles. *e-Journal of Surface Science and Nanotechnology*. 4:439-442.
- [8] Qiu HS, Gao J, Ma B, Zhang ZZ, Jin QY. 2006. Spin reorientation transition and its gas absorption effect on Ni/fct-Fe films at 110 K. *Journal of Korean Physical Society*. 49:2095-2098.
- [9] Yokoyama T, Matsumura D, Amemiya K, Kitagawa S, Suzuki N, Ohta T. 2003. Spin reorientation transitions of ultrathin Co/Pd(111) films induced by chemisorption: x-ray magnetic circular dichroism study. *Journal of Physics: Condensed Matter*. 15:S537-S546.
- [10] Salehi A, Nazerian V. 2007. Characterization of magnetic Ni/n-Si Schottky contact for hydrogen gas sensing applications. *Sensors and Actuators B*. 122:572-577.

- [11] Fuchs GD, Emley NC, Krivorotov IN, Braganca PM, Ryan EM, Kiselev SI, Sankey JC, Katine JA, Ralph DC, Buhrman RA. 2004. Spin-transfer effects in nanoscale magnetic tunnel junctions. *Applied Physics Letters*. 85:1205-1207.
- [12] Moodera JS, Kinder LR, Wong TM, Meservey R. 1995. Large magnetoresistance at room temperature in ferromagnetic thin film tunnel junctions. *Physical Review Letters*. 74:3273-3276.
- [13] Petta JR, Slater SK, Ralph DC. 2004. Spin-dependent transport in molecular tunnel junctions. *Physical Review Letters*. 93:136601-1–136601-4.
- [14] Bass J, Schroeder PA, Pratt WP Jr, Lee SF, Yang Q, Holody P, Henry LL, Loloee R. 1995. Studying spin-dependent scattering in magnetic multi layers by means of perpendicular (CPP) magneto resistance measurements. *Materials Science and Engineering B*. 31:77-83.
- [15] Waintal X, Myers EB, Brouwer PW, Ralph DC. 2000. Role of spin-dependent interface scattering in generating current-induced torques in magnetic multilayers. *Physical Review B*. 62:12317-12327.
- [16] Penn DR, Stiles MD. 2005. Spin transport for spin diffusion lengths comparable to mean free paths. *Physical Review B*. 72:212410-1–212410-4.
- [17] Bozec D, Howson MA, Hickey BJ, Shatz S, Wiser N, Tsybmal EY, Pettifor DG. 2000. Mean free path effects on the current perpendicular to the plane magneto resistance of magnetic multi layers. *Physical Review Letters*. 85:1314-1317.
- [18] Zutic I, Fabian J, Sarma SD. 2004. Spintronics: fundamentals and applications. *Reviews of Modern Physics*. 76:323-410.
- [19] Schep KM, Kelly PJ, Bauer GEW. 1998. Giant magnetoresistance and electronic structure. *Physical Review B*. 57:8907-8926.
- [20] Tsybmal EY, Pettifor DG. 1997. Modelling of spin-polarized electron tunnelling from 3d ferromagnets. *Journal of Physics: Condensed Matter*. 9:L411-L417.
- [21] Salehi A, Nikfarjam A, Kalantari DJ. 2006. Pd/porous-GaAs Schottky contact for hydrogen sensing application. *Sensors and Actuators B*. 113:419-427.